On the acoustic properties of CsD_2PO_4 and RbD_2PO_4 crystals near phase transitions under hydrostatic pressure

On the acoustic properties of CsD_2PO_4 and RbD_2PO_4 crystals near phase transitions under hydrostatic pressure

A V Kityk†, Ya I Shchur‡, L P Lutsiv-Shumskii† and O G Vlokh†‡

† Lviv State I Franko University, Universitetska Street 1, Lviv, 290602, Ukraine
‡ Institute of Physical Optics, Dragomanova 19, Lviv, 290005, Ukraine

Abstract. The influence of hydrostatic pressure on the temperature behaviour of acoustic properties in the vicinity of phase transitions of CsD_2PO_4 and RbD_2PO_4 crystals is studied. The pressure–temperature phase diagrams are obtained. The results are considered within the framework of phenomenological theory.

1. Introduction

Monoclinic crystals of a caesium deuterium phosphate (CsD_2PO_4; DCDP) and rubidium deuterium phosphate (RbD_2PO_4; DRDP) belong to the low-symmetry representatives of KH_2PO_4-type ferroelectrics. At atmospheric pressure DCDP crystals undergo a phase transition (PT) at $T_C = 265$ K from the high-temperature normal (N) phase (space group $P2_1/m$) with two molecular units per unit cell to the ferroelectric (F) phase (space group $P2_1$) with the spontaneous polarization along the b axis (Senningsen and Thomas 1978, Itoh *et al* 1983). Under the action of hydrostatic pressure the PT point T_C shifts considerably to the low-temperature region (Gesi and Ozawa 1978). This is caused by an increase of the frequency of deuteron tunnelling on the hydrogen bonds. It has also been found that the N–F PT line in the pressure–temperature (P–T) phase diagram of DCDP crystals changes at the triple point ($P_t = 590$ MPa, $T_t = 213$ K (Gesi and Ozawa 1978); $P_t = 545$ MPa, $T_t = 218$ K (Marchon and Novak 1984)) into a line of N–antiferroelectric (AF) PT. In the AF phase the unit-cell dimension is doubled along the a axis compared with that in the N phase.

DCDP crystals are characterized by the presence of two types of hydrogen bonds linking PO_4 tetrahedra (Iwata *et al* 1980, Frazer *et al* 1979). The O–D(1) bonds link the PO_4 groups along the a axis and they are ordered in the N phase. The shorter O–D(2) bonds form zigzag quasi-one-dimensional chains along the b axis. In the N phase they are disordered, while in the F and AF phases they become ordered. Critical phenomena associated with the N–F and N–AF PT in DCDP crystals have been studied by x-ray diffraction (Itoh *et al* 1983), neutron scattering (Semmingson *et al* 1977, Youngblood *et al* 1980, Iwata *et al* 1980, Frazer *et al* 1979) and Raman scattering (Wada *et al* 1979, Kasahara *et al* 1984, Marchon and Novak 1984). However, the origin of such a polycritical point in this compound is not yet completely clear, and new experimental methods can supply important additional information.

DRDP crystals at atmospheric pressure undergo two successive PT from the high-temperature N phase (space group $P2_1/m$) at $T_1 = 377$ K and $T_2 = 317$ K. Between T_1 and T_2 this system exhibits monoclinic symmetry (space group $P2_1/c$) and the unit-cell

dimension is doubled along the c axis (Hagiwara *et al* 1984). Below T_2 the ferrielectric (FI) phase has also been identified as monoclinic (space group $P2_1$) and the spontaneous polarization is parallel to the b axis (Suzuki *et al* 1983). The unit cell in the low-temperature phase is doubled simultaneously along both c and a axes with respect to the N phase ($T > T_1$). The intermediate (IM) phase in DRDP is isostructural to the antiferroelectric phase in DCDP compounds. The low-temperature phase in DRDP appears as a result of deuterons ordering on the hydrogen bonds parallel to the b axis. The PT in these crystals have been studied earlier by dielectric (Sumita *et al* 1981, Komukae and Makita 1985) and acoustic (Yakushkin 1986) measurements.

Gesi *et al* (1983) and Baranov *et al* (1985) have investigated the P–T phase diagram of DRDP. Quite different P–T phase diagrams have been obtained by these authors using the same method of dielectric measurements. Particularly, Baronov *et al* (1985) have found two triple points in the P–T phase plane, while Gesi *et al* (1983) have revealed only gradually decreasing T_1 and T_2 PT points under hydrostatic pressure. This disagreement is considered in detail in the present work, where the P–T phase diagram of DRDP crystals was obtained using acoustic measurements. The results are considered within the framework of the phenomenological theory.

2. Experiment

The deuterium concentration of the DCDP and DRDP specimens used in this work was estimated as 98% assuming a linear relation between the Curie temperature and the deuterium concentration. We use the following crystallographic orientation for both crystals in the N phase: $a > b > c$. The specimens were prepared for studying ultrasonic waves (USW) propagating along X, Y and Z axis, where $Y \parallel b$, $Z \parallel c$ and $X \perp bc$.

Velocities of the transverse and longitudinal USW ($f = 10$ MHz) were measured by the pulse–echo overlap method (Papadakis 1967) with an accuracy of the order of 10^{-4}–10^{-5}. The accuracy of absolute velocity determination was about 0.5%. Ultrasonic attenuation was determined from the decay rate of echo pulses with an accuracy of about 10%. Acoustic investigations under applied hydrostatic pressure have been performed in the region from 0.1 to 600 MPa and 160–400 K using a high-pressure camera.

3. Experimental results

3.1. Caesium deuterium phosphate

Figures 1–4 indicate the temperature dependences of the velocities and attenuations of the pure longitudinal $V_2(q \parallel Y, E \parallel Y)$, quasilongitudinal $V_1(q \parallel X, E \parallel X)$, pure transverse $V_6(q \parallel Y, E \parallel XZ)$ and quasi-transverse $V_5(q \parallel X, E \parallel Z)$ USW in DCDP crystals at different hydrostatic pressures (here q is USW vector, E is its polarization). The polydomain specimen shows a clear decrease of the V_2 velocity, while the corresponding attenuation coefficient α_2 (figure 1, insert) possesses an anomalous peak immediately below T_C. Under hydrostatic pressure, ferroelectric PT temperature T_C is shifted to the low-temperature region and the values of the anomalous V_2 and $\Delta\alpha_2$ changes near T_C show some increase. In the high-pressure region the V_2 temperature dependence shows a jump near the F–AF PT temperature T_{CA} (curves C and D). Under applied pressure, the F phase becomes narrower and finally disappears at $P_t = 575$ MPa. Only a clear kink of $V_2(T)$ is observed at $P \geqslant P_t$ in the region of the direct N–AF PT temperature T_A. Note that the monodomain specimens near

T_C show the temperature dependences of V_2 and α_2, which differ essentially from those in polydomain ones (figure 1). The monodomain state has been realized at each temperatue and pressure by applying an electric field $E \sim 100$ V cm^{-1} along the b axis and then reducing it to zero. No large softening but only insignificant kinks of $V_2(T)$ are observed in that case in the vicinity of the N–F PT.
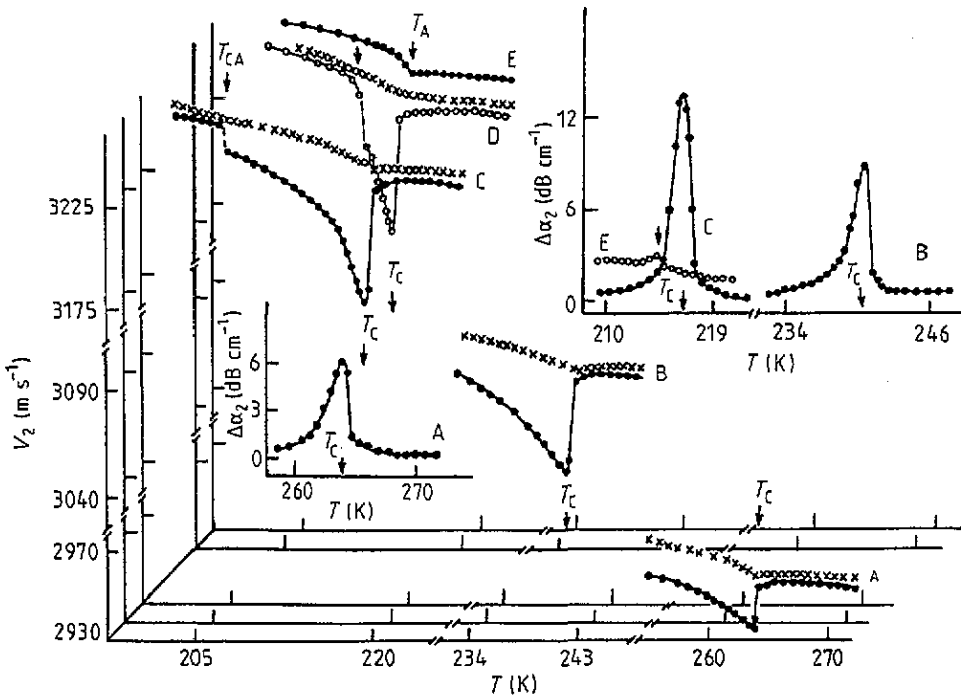

Figure 1. The temperature dependence of the pure longitudinal USW velocity V_2 and attenuation $\Delta\alpha_2$ at different pressures of DCDP crystals: curve A, 0.1 MPa; curve B, 280 MPa; curve C, 540 MPa; curve D, 560 MPa; curve E, 580 MPa. (×) curves A–D, $E = 50$ V cm^{-1} ($E \parallel Y$).

The isobaric temperature dependences of the transverse USW V_6 are shown in figure 2. In the low-pressure region $V_6(T)$ dependences are linear in the N phase. Here the N–F PT is accompanied by clear kinks on these curves. At high pressures the linear character of the $V_6(T)$ temperature dependences is lost in the temperature range T_C to $T_C + 6$ K of the N phase, and only an insignificant and smooth kink of $V_6(T)$ is observed near PT point T_A at $P \geqslant P_t$.

In the low-pressure region the temperature dependences of the USW velocities V_1 (figure 3) and V_5 (figure 4) and corresponding attenuation coefficients α_1 and α_5 near T_C are quite similar to those of USW V_2 and α_2, while at high pressures, in the vicinity of the triple point, some peculiarities of these dependences occur. Particularly, an essential decrease of V_5 USW velocity and increase of attenuation α_5 are clearly observed already in the N phase at 5–7 K above T_C ($P < P_t$) or T_A ($P \geqslant P_t$). Besides, both USW velocities V_1 and V_5 undergo a jump-like decrease in the region of the N–AF PT, while the corresponding attenuation coefficients α_1 and α_5 increase significantly here.

Figure 5 shows the temperature dependences of the effective electroacoustic coefficient $f_{222}^* = f_{222}/2C_{22} = \Delta V_2/V_2\Delta E_2$ (C_{22} is the elastic constant) at different pressures. In that
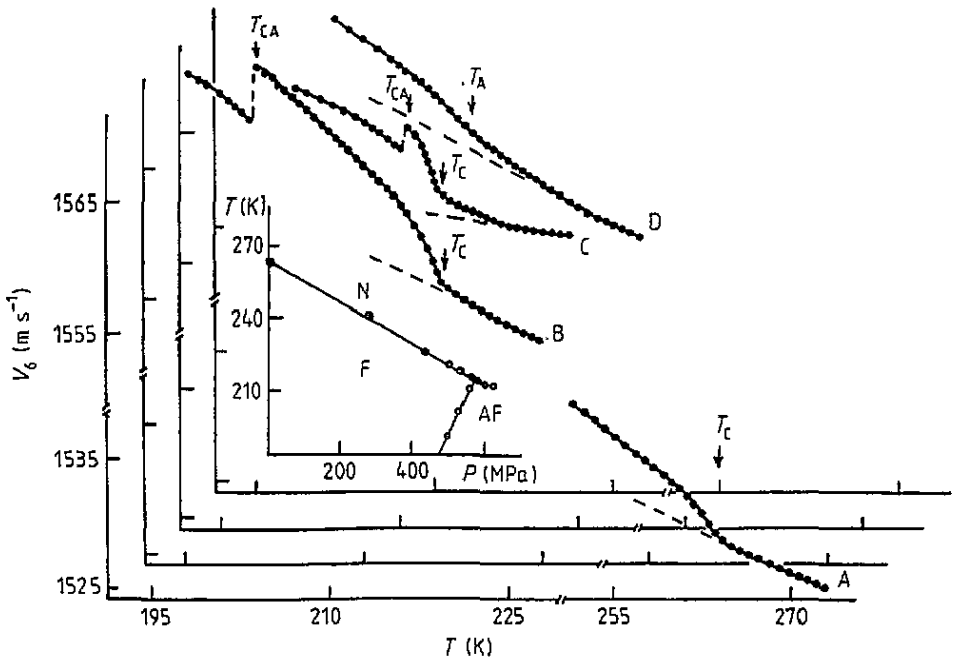
Figure 2. The temperature dependence of the pure transverse USW velocity V_6 at different pressures of DCDP crystals: curve A, 0.1 MPa; curve B, 530 MPa; curve C, 560 MPa; curve D, 580 MPa. The insert shows the $P-T$ phase diagram of DCDP crystals, showing N, F and AF phases.

case the USW vector q and applied electric field $E_2 \sim 200$ V cm^{-1} were parallel to the b axis. The linear electroacoustic effect practically has not been observed in the N phase far from PT point T_C. Obviously this is caused by the centre of symmetry that is available in the N phase. The clear anomalous peak of the $f^*_{222}(T)$ dependences is observed in the region of the N–F PT. The value of the f^*_{222} maximum at T_C essentially decreases under the action of hydrostatic pressure. In the high-pressure region, two maxima in the f^*_{222} temperature dependences are observed near both T_A and T_{CA} PT points (figure 5, curve E), while the linear electroacoustic effect has not been detected in N and AF phase at $P \geqslant P_t$.

3.2. Rubidium deuterium phosphate

The temperature dependences of the pure longitudinal $V_2(q \parallel Y, E \parallel Y)$, pure transverse $V_4(q \parallel Y, E \parallel XZ)$, quasi-longitudinal $V_1(q \parallel X, E \parallel X)$ and the quasi-transverse $V_5(q \parallel X, E \parallel Z)$ USW velocities of DRDP crystals at different hydrostatic pressures are presented in figures 6–9 respectively.

A visible decrease of the longitudinal USW velocity V_2 (figure 6) is observed already ~ 20–25 K above T_1 in the N phase at atmospheric pressure, which clearly indicates the significant fluctuation effects in this compound. In the vicinity of PT temperatures T_1 and T_2 the USW velocity V_2 essentially decreases, which is in good agreement with previous studies performed by Yakushkin (1986).

The PT temperatures T_1 and T_2 both shift to the low-temperature region under applied hydrostatic pressure. However, the character of the temperature dependences of USW velocity V_2 practically does not change in that case. Only the temperature range of the
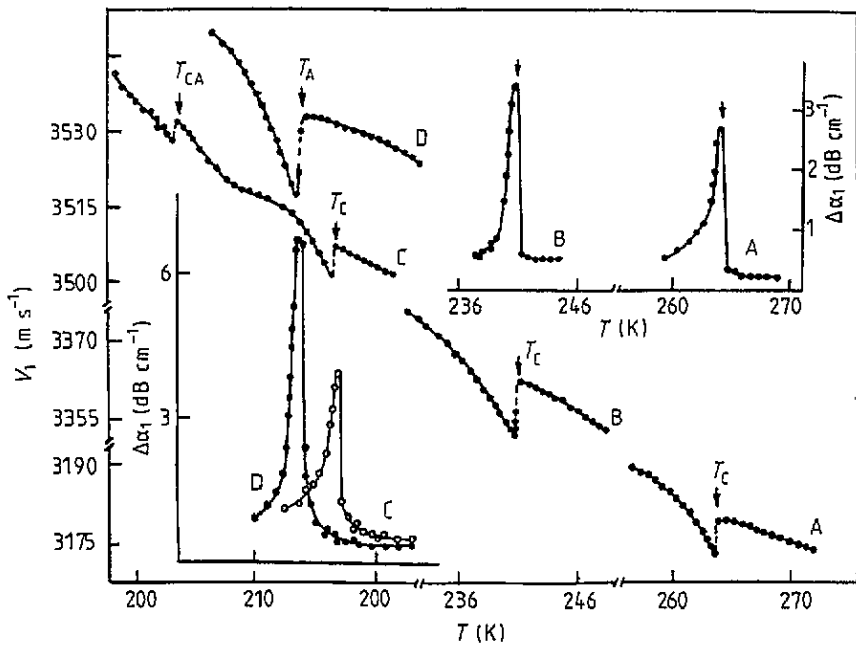
Figure 3. The temperature dependence of the quasi-longitudinal USW velocity V_1 and attenuation $\Delta\alpha_1$ at different pressures of DCDP crystals: curve A, 0.1 MPa; curve B, 280 MPa; curve C, 540 MPa; curve D, 580 MPa.

Figure 4. The temperature dependence of the quasi-transverse USW velocity V_5 and attenuation $\Delta\alpha_5$ at different pressures of DCDP crystals: curve A, 0.1 MPa; curve B, 280 MPa; curve C, 550 MPa; curve D, 580 MPa.
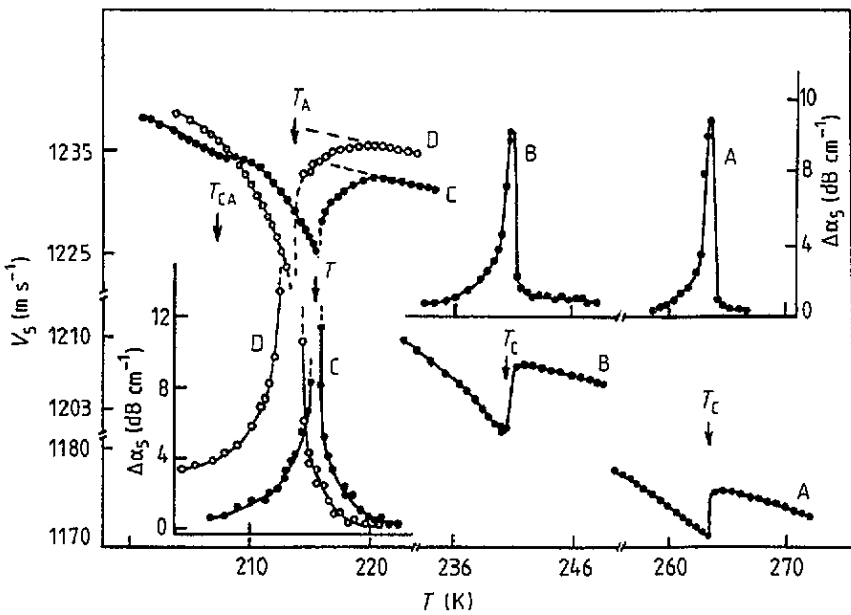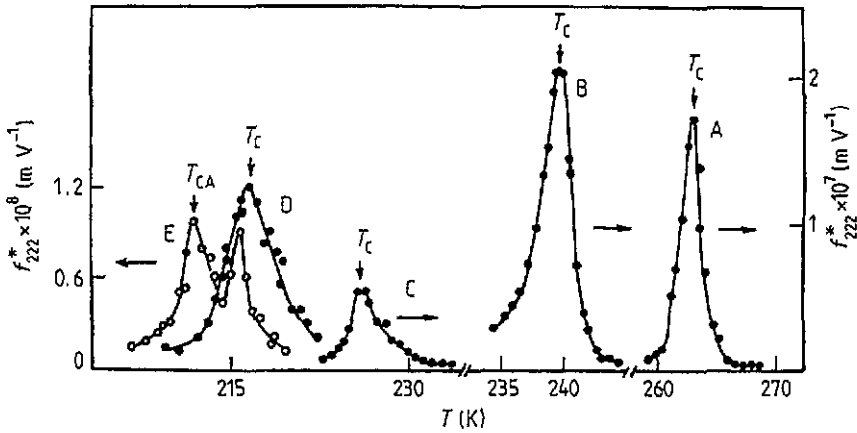
Figure 5. The temperature dependence of effective electroacoustic coefficient f_{222}^* at different pressures of DCDP crystals: curve A, 0.1 MPa; curve B, 275 MPa; curve C, 440 MPa; curve D, 540 MPa; curve E, 560 MPa.

Figure 6. The temperature dependence of pure longitudinal USW velocity V_2 at different pressures of DRDP crystals: curve A, 0.1 MPa; curve B, 175 MPa; curve C, 295 MPa; curve D, 385 MPa; curve E, 495 MPa.

IM phase becomes somewhat narrower. Jump-like decreases of the quasi-longitudinal V_1 (figure 7) and quasi-transverse V_5 (figure 8) USW velocities are also observed near both PT temperatures, while the temperature dependences of the pure transvese USW velocity
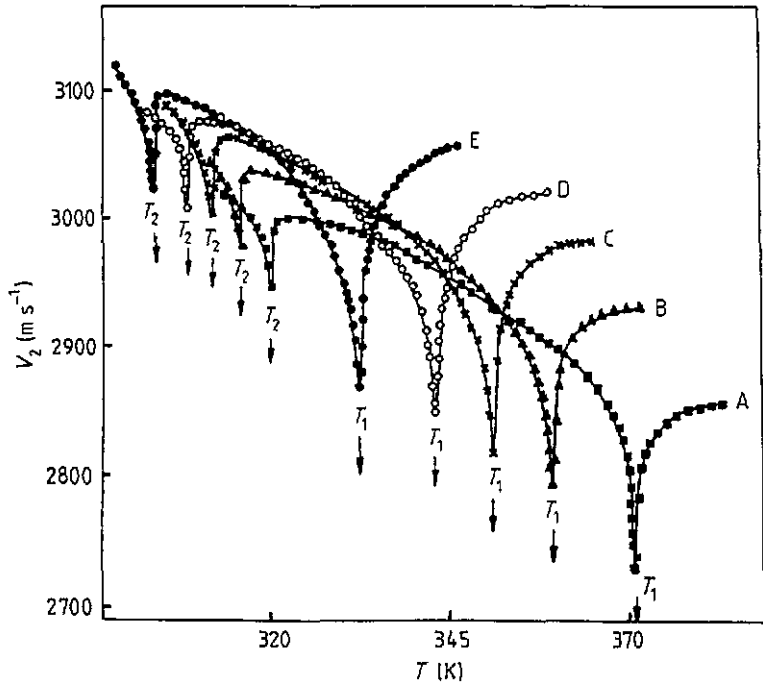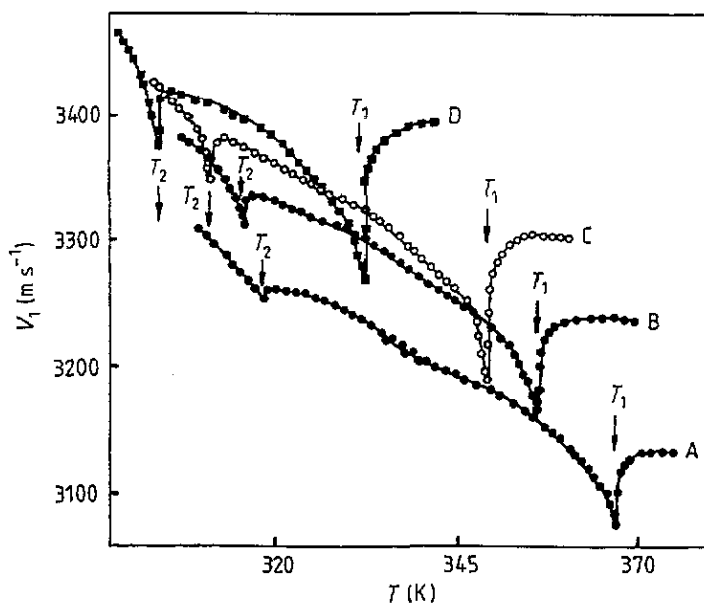
Figure 7. The temperature dependence of the quasi-longitudinal USW velocity V_1 at different pressures of DRDP crystals: curve A, 45 MPa; curve B, 205 MPa; curve C, 315 MPa; curve D, 495 MPa.

V_4 (figure 9) possesses near this PT only clear kinks. Note that no additional anomalies have been observed between T_1 and T_2 at high pressures up to 500 MPa in the temperature dependences of USW velocities V_1, V_2, V_4 and V_5. The P–T phase diagram of DRDP compounds obtained in the present work from acoustic measurements (figure 10) in this sense is in good agreement with those obtained from dielectric measurements by Gesi *et al* (1983).

4. Discussion

Using Cristofel's equation we have obtained the following relations between USW velocities V_i and elastic constants C_{ij}:

$$\rho V_2^2 = C_{22} \qquad 2\rho V_6^2 = C_{44} + C_{66} + [(C_{44} - C_{66})^2 + 4C_{46}^2]^{1/2} \tag{1a}$$

$$2\rho V_4^2 = C_{44} + C_{66} - [(C_{44} - C_{66})^2 + 4C_{46}^2]^{1/2} \tag{1b}$$

$$2\rho V_1^2 = C_{11} + C_{55} + [(C_{11} - C_{55})^2 + 4C_{15}^2]^{1/2} \tag{2a}$$

$$2\rho V_5^2 = C_{11} + C_{55} - [(C_{11} - C_{55})^2 + 4C_{15}^2]^{1/2} \tag{2b}$$

where ρ is the crystal density. The phenomenological description of the acoustic anomalies near the PT in the Landau theory framework is based on the free-energy expansion with coupling terms, which correspond to anharmonic interactions between the strains U_1–U_6 and the order parameter. Using a standard procedure (see the example Rehwald 1973) the contributions to the elastic constant, caused by the PT, may be easily obtained from the free energy.
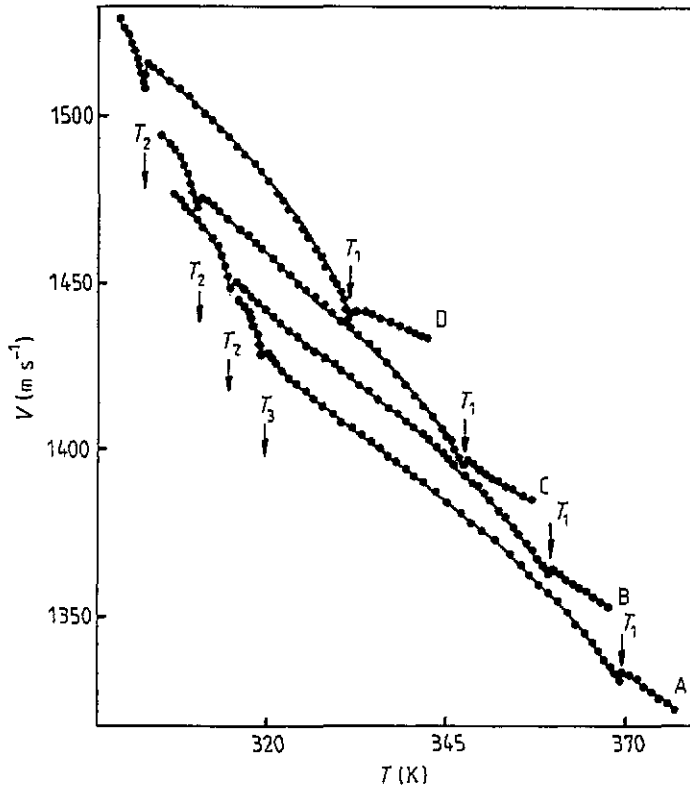
Figure 8. The temperature dependence of the quasi-transverse USW velocity V_5 at different pressures of DRDP crystals: curve A, 0.1 MPa; curve B, 165 MPa; curve C, 315 MPa; curve D, 495 MPa.

4.1. Free energy

The PT in DCDP and DRDP crystals are associated with the different soft modes condensed in the centre ($q_7 = 0$) or at the boundary ($q_{11} = \frac{1}{2}b_1$, $q_{13} = \frac{1}{2}b_3$) of the Brillouin zone (here b_1, b_3 are the reciprocal lattice parameters, and Kovalev's notation (Kovalev 1986) has been used for the identification of wavevectors). Group-theory consideration shows that the irreducible representations of the $P2_1/m$ space group have the same form for all these Brillouin zone points. There are four one-dimensional irreducible representations for this group (see table 1). According to this the order parameters in all corresponding cases contain only one component. The invariants in the free energy have been constructed in the usual way, where the wavevectors of the corresponding interacting normal phonon coordinates have satisfied the condition $\sum q_i = 0$ or G, where $G = m_1 b_1 + m_2 b_2 + m_3 b_3$ (m_1, m_2, m_3 are integers).

4.1.1. Caesium deuterium phosphate. Using table 1 it is easy to show that the irreducible representation A_u is responsible for the PT into F or AF phases in DCDP compounds. The relevant part of the free energy in both cases, expressed directly in normal-mode coordinates $P(q_7 = 0) \in A_u$ and $Q(q_{11} = \frac{1}{2}b_1) \in A_u$ can be written as
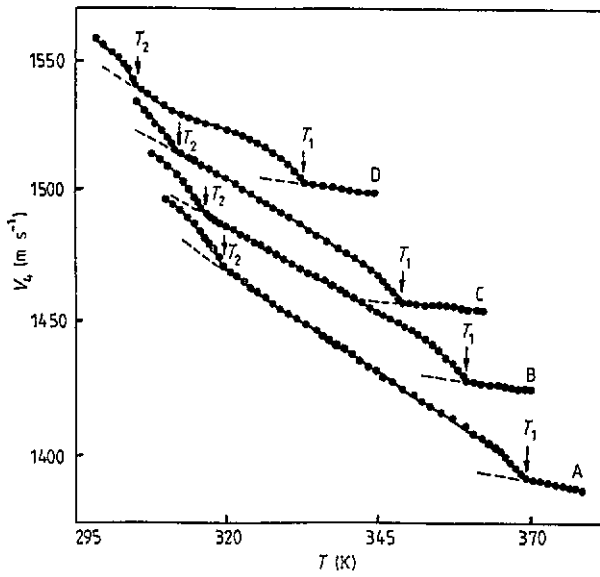
Figure 9. The temperature dependence of the pure transverse USW velocity V_4 at different pressures of DRDP crystals: curve A, 0.1 MPa; curve B, 155 MPa; curve C, 295 MPa; curve D, 495 MPa.
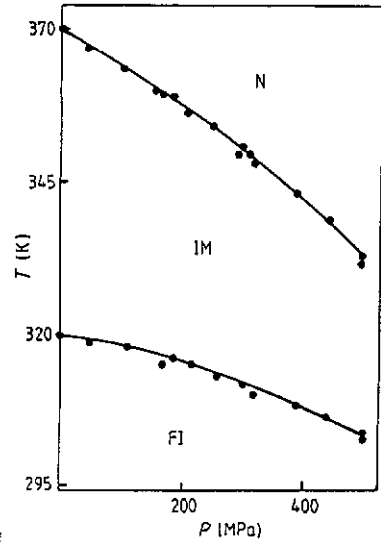
Figure 10. The P–T phase diagram of DRDP crystals, showing N phase ($P2_1/m$), IM phase ($P2_1/c$) and FI phase ($P2_1$).

Table 1. The irreducible representations of $P2_1/m$ space group in the Brillouin zone points $q_7 = 0$, $q_{11} = b_1/2$, $q_{13} = b_3/2$, and of $P2_1/c$ space group at $q_{11} = b_1/2$.

	$\{E\vert000\}$	$\{C_{2y}\vert0\tfrac{1}{2}0\}$	$\{\sigma_y\vert0\tfrac{1}{2}0\}$	$\{I\vert000\}$
A_g	1	1	1	1
B_g	1	-1	-1	1
A_u	1	1	-1	-1
B_u	1	-1	1	-1

$$F_F = \tfrac{1}{2}\omega_P^2(0)P^2 + \tfrac{1}{4}\beta_P P^4 + \sum_{i=1}^{3} a_{Pi} P^2 U_i + \tfrac{1}{2}\sum_{i,j=1}^{3} b_{Pij} P^2 U_i U_j + \tfrac{1}{2}\sum_{j=4}^{6} b_{Pjj} P^2 U_j^2$$

$$+ a_{P5} P^2 U_5 + \tfrac{1}{2}\sum_{i=1}^{3} b_{Pi5} P^2 U_i U_5 + \tfrac{1}{2}b_{P46} P^2 U_4 U_6 \qquad \text{(F phase)} \qquad (3)$$

$$F_{AF} = \tfrac{1}{2}\omega_Q^2(q_{11})Q^2 + \tfrac{1}{4}\beta_Q Q^4 + \sum_{i=1}^{3} a_{Qi} Q^2 U_i + \tfrac{1}{2}\sum_{j=4}^{6} b_{Qjj} Q^2 U_j^2 + a_{Q5} Q^2 U_5$$

$$+ \tfrac{1}{2}\sum_{i=1}^{3} b_{Qi5} Q^2 U_i U_5 + \tfrac{1}{2}b_{Q46} Q^2 U_4 U_6 \qquad \text{(AF phase)} \qquad (4)$$

$$F_{P,Q} = \gamma Q^2 P^2 \qquad (5)$$

where $\omega_P^2(0) = A_P(T - T_C)$ and $\omega_Q^2(q_{11}) = A_Q(T - T_A)$ are the soft-mode frequency squared at the centre or boundary of the Brillouin zone, and U_i are strain components.

As usual we assume that the all free-energy expansion coefficients A_P, A_Q, β_P, β_Q, a_{Pi}, a_{Qi}, b_{Pij} and b_{Qij} are positive. Note that both P and Q modes belong to the same phonon branch. Freezing of the P mode in the centre of the Brillouin zone leads to the appearance of macroscopic spontaneous polarization, while the condensation of the Q mode at the Brillouin zone boundary is accompanied by the appearance of antipolarization. Phenomenologically $\omega_P(0)$ and $\omega_Q(q)$ are connected, which directly follows from Kittel's theory. According to this theory the harmonic part of the free energy is presented as follows:

$$F = f(P_a^2 + P_b^2) + g P_a P_b \qquad (6)$$

where P_a and P_b are polarizations in the neighbouring sublattices. As was shown earlier by Smolenskiy *et al* (1985), both considerations are equivalent if one takes into account that $P \equiv P_a + P_b$, $Q \equiv P_a - P_b$, $\omega^2(0) = f - g/2$ and $\omega^2(q_{11}) = f + g/2$. Particularly the PT from the N phase to the F phase takes place if $f - g/2 = 0$ and $f + g/2 > 0$, while the PT into the AF phase is realized if $f + g/2 = 0$ and $f - g/2 > 0$. The triple point on the P–T phase diagrams satisfied the condition when $f = 0$ and $g = 0$.

4.1.2. Rubidium deuterium phosphate. The PT in DRDP from the N to the IM phase is connected with the condensation of the soft mode at the Brillouin zone boundary in the point $q_{13} = \frac{1}{2}b_3$. From table 1 it follows that the soft mode transforms according to the irreducible representation A_u. Consequently the free energy in that case has a form quite similar to equation (4). A more complicated situation takes place for the PT from the IM to the FI phase. It is impossible to explain the appearance below T_2 of the uncompensated homogeneous polarization by the condensation only of the single soft mode at $q_{11} = \frac{1}{2}b_1$. Note that this transition is of second order. Taking into account that the irreducible representations of $P2_1/c$ space group at $q_{11} = \frac{1}{2}b_1$ correspond to table 1, the PT into the FI phase may be explained by the simultaneous condensation near T_2 of two modes $R(q_{11}) \in B_g$ and $S(q_{11}) \in B_u$. This assumption adequately describes the symmetry changes and appearance of the small homogeneous polarization along the b-axis as well. The equilibrium value of the spontaneous polarization follows from the part of the free energy $F_{P,R,S}$ that includes terms in the polarization P_y both alone and in combination with R and S. In the low-order approximation $F_{P,R,S}$ may be written as

$$F_{P,R,S} = \gamma_0 P_y S R + \gamma_1 P_y^2 + \gamma_2 P_y^2 S^2 + \gamma_3 P_y^2 R^2 - P_y E_y. \qquad (7)$$

Assuming that no external electric field is present ($E_y = 0$), after the minimization of equation (7) with respect to P_y we obtain

$$P_{y0} = -\frac{\gamma_0 S_0 R_0}{2(\gamma_1 + \gamma_2 S_0^2 + \gamma_3 R_0^2)}. \qquad (8)$$

Obviously, it is clear from equation (8) that the macroscopic spontaneous polarization P_{y0} appears only as the result of simultaneous condensation of two soft modes when the equilibrium values of S_0 and R_0 differ from zero.

Let us consider the free-energy expansion including both S and R normal-phonon coordinates and strain components U_i. Using table 1 we obtain

$$F = F_R + F_S + F_{R,S} + F_{R,S,U} \qquad (9)$$

$$F_R = \omega_R^2(q_{11})R^2 + \beta_R R^4 + \cdots \qquad (9a)$$

$$F_S = \omega_S^2(q_{11})S^2 + \beta_S S^4 + \cdots \tag{9b}$$

$$F_{R,S} = \epsilon S^2 R^2 \tag{9c}$$

$$F_{R,S,U} = \sum_{i=1}^{3}(a_{Ri}R^2 + a_{Si}S^2)U_i + \tfrac{1}{2}\sum_{i,j=1}^{3}(b_{Rij}R^2 + b_{Sij}S^2)U_iU_j$$

$$+ \tfrac{1}{2}\sum_{j=4}^{6}(b_{Rjj}R^2 + b_{Sjj}S^2)U_j^2 + (a_{R5}R^2 + a_{S5}S^2)U_5$$

$$+ \tfrac{1}{2}\sum_{i=1}^{3}(b_{Ri5}R^2 + b_{Si5}S^2)U_iU_5 + \tfrac{1}{2}(b_{R46}R^2 + b_{S46}S^2)U_4U_6 \tag{9d}$$

where $\omega_R^2(q_{11}) = A_R(T - T_R)$, $\omega_S^2(q_{11}) = A_S(T - T_S)$ and we assume that $T_R \simeq T_S \simeq T_2$.

4.2. Acoustic anomalies

The changes of the complex elastic constant in the region of the PT directly follow from the well known relation (see for example the review article by Rehwald (1973))

$$\Delta C_{ij}^* = \frac{\partial^2 F}{\partial U_i \partial U_j} - \frac{1}{1 + i\Omega\tau}\frac{\partial^2 F}{\partial\eta\partial U_i}\left|\frac{\partial^2 F}{\partial\eta^2}\right|^{-1}\frac{\partial^2 F}{\partial\eta\partial U_j} \tag{10}$$

where $\Omega = qV = 2\pi f$ is the USW frequency, τ is the soft-mode relaxation time and η is the order parameter. Here the first term corresponds to the contribution only to the real part of the elastic constant, while the second one reveals the relaxation mechanism of the Landau–Khalatnikov type. Using equations (3), (4), (9) and (10) we obtain

$$\Delta C_{ii}^* = b_{\eta ii}\eta_0^2 - a_{\eta i}^2\eta_0^2/[\omega_\eta^2(1 + i\Omega\tau_\eta)] \qquad i = 1, 2, 3, 5 \tag{11a}$$

$$\Delta C_{66}^* = b_{\eta 66}\eta_0^2 \qquad \Delta C_{44}^* = b_{\eta 44}\eta_0^2$$

$$\Delta C_{46}^* = \tfrac{1}{2}b_{\eta 46}\eta_0^2 \qquad \Delta C_{15}^* = \tfrac{1}{2}b_{\eta 15}\eta_0^2 \tag{11b}$$

where $\eta_0^2 = -A_\eta(T - T_\eta)/2\beta_\eta$ is the equilibrium value of the corresponding normal-phonon coordinates (P_0, Q_0, R_0 or S_0), $T_\eta(T_C, T_A, T_1, T_2)$ and $\tau_\eta(\tau_P, \tau_Q, \tau_R$ or $\tau_S)$. One must note that $P_0 \neq 0$ only in the F phase of DCDP, $Q_0 \neq 0$ only in the AF phase of DCDP or in the IM and FI phases of DRDP and finally both $R_0 \neq 0$ and $S_0 \neq 0$ only in the FI phase of DRDP. Using such a generalized and reduced form of equation (11) it is easy to give the qualitative analysis of acoustic anomalies near all the PT for both compounds.

It follows from equations (1), (2) and (11) that USW velocities V_1, V_2 and V_5 should exhibit a sudden decrease at second-order PT T_C, T_A, T_1 and T_2, while the corresponding attenuation coefficients essentially increase here, which is caused by the second term of equation (11a) and follows from the third-order anharmonic interaction between strains and soft modes. This is observed experimentally (figures 1,3,4 and 6–8). The changes in these USW velocities below T_η are caused by the contributions of the first term of equations (11a) and (11b). This fourth-order anharmonicity leads to quadratic dependences of V_i on the order parameter at $T < T_\eta$.

The temperature changes in the pure transverse USW velocity V_4 and V_6 near all the considered PT points are caused only by the fourth-order anharmonicity, which gives a

contribution only to the real part of the complex elastic constant. Consequently clear kinks on the $V_4(T)$ (figure 9) and $V_6(T)$ (figure 2) dependences appear in the region of T_1, T_2 (DRDP) and T_C, T_A (DCDP) respectively, while anomalous attenuation is quite absent here. Note that the step-like changes of V_6 USW velocity at PT point T_{CA} in DCDP is caused by the first-order character of this transition.

In the N phase $\eta_0 = 0$ and consequently no contribution to the elastic properties associated with PT should be observed above T_C (DCDP) or T_1 (DRDP). As can be clearly seen from the experimental data, only in the low-pressure region in the case of DCDP crystals do all USW velocities depend linearly on the temperature, while the attenuation is absent. At the same time, as was pointed out above, at high pressures near the triple point in DCDP or in the region of T_1 in DRDP the USW velocities are not linear already far from the PT points and anomalous attenuation increases significantly here. This 'unexpected' temperature behaviour of acoustic properties is obviously caused by the fluctuation effects. It is known that in the case of uniaxial proper ferroelectrics the macroscopic electric field, which appears as a result of the correlation of polarization fluctuations, leads to its decrease in the PT region (Levanyuk *et al* 1968). Consequently, in the low-pressure region in the N phase of DCDP crystals the temperature dependences of V_i are linear and anomalous attenuation is absent. At high pressures in the vicinity of the triple point, the antipolarization fluctuations essentially increase. These fluctuations, in spite of the polarization ones, are not diminished, since the polarization in the neighbouring sublattice has antiparallel orientation and the electric field is short-ranged. That is why at high pressure we obtain a significant increase of the fluctuation contribution to acoustic properties. Note that the fluctuation of antipolarization in the vicinity of the triple point in DCDP crystals has also been observed earlier in Raman spectra (Marchon and Novak 1984).

Using the experimental values of the negative velocity jump ΔV_2 and anomalous attenuation $\Delta\alpha_2$ (figure 1) we have determined the soft-mode relaxation time τ_P in DCDP crystals at atmospheric pressure. For this aim we take into account the well known relation $\Delta\alpha_2 = (\Delta V_2/V_2)\Omega^2\tau_P$. From the analysis of experimental results it follows that $\tau_P = \tau_{P0}/(T_C - T)$, where $\tau_{P0} = (5 \pm 0.5) \times 10^{-9}$ K s. The obtained value of τ_{P0} is more than of one order higher than that in the case of CDP, determined in a similar way by Kanda *et al* (1983). Unfortunately the relaxation times were not determined in all other cases since the fluctuation effects become significant.

4.3. Influence of electric field on acoustic properties in DCDP

Experimental results clearly show that an electric field applied along the ferroelectric axis changes essentially the acoustic behaviour near the N–F PT. Particularly, a sudden decrease in V_2 near T_C in the case of a polydomain specimen (figure 1) disappears after its 'monodomainizing' by external fields $E_y \sim 50$–100 V cm^{-1}. Quite a similar situation has been earlier observed in CDP by Kanda *et al* (1983). We explain this result in the following way. The relaxation time of the order parameter in the F phase increases significantly on approaching the F–N PT. The USW changes the order parameter and consequently changes the macroscopic electric field caused by the long-range dipole–dipole interactions. In connection with that, the relaxation time of polarization diminishes the critical increase near T_C and anomalies of longitudinal USW velocity V_2 and attenuation α_2 become suppressed. According to Geguzina and Krivoglaz (1967), such a situation is realized if USW length $\lambda \ll R_D$, where R_D is the Debye radius of screening, or in the case of ferroelectric crystals if $\lambda \ll d$, where d is the domain size along the b axis. On the contrary, in a polydomain specimen ($\lambda \gg d$) the acoustic anomalies are preserved. It is in good agreement with the experimental data.

Let us consider the anomalous behaviour of electroacoustic effect near the N–F PT in DCDP crystals. The relevant additional contribution to the free energy contains the normal-phonon coordinate P, the induced polarization $P_2^* = \epsilon_0 \epsilon_2 E_2$ and the strain component U_2:

$$\Delta F = a_{P2} P P_2^* U_2 + \tfrac{1}{2} b_{P22} P P_2^* U_2^2 + \tfrac{1}{2} b_{P22} P_2^{*2} U_2^2. \tag{12}$$

Note that the electrostrictive contribution to the elastic properties in the case of a monodomain specimen is suppressed and consequently the first term in equation (12) will not be taken into account. Using the standard procedure we obtain

$$\Delta f_{222}^* = (b_{P22}/2C_{22})[P_0 \epsilon_0 \epsilon_2 + 2(\epsilon_0 \epsilon_2)^2 E_2] \tag{13}$$

From equation (13) it follows that in the N phase at $E_2 \to 0$ the coefficient of the linear electroacoustic effect $f_{222}^* \to 0$, which is caused by the availability of a symmetry centre in this phase. As a matter of fact the electroacoustic effect here is quadratic. At $E_2 = \text{const}$ the changes Δf_{222}^* in the N phase are caused only by the temperature dependence of dielectric permittivity ($\Delta f_{222}^* \sim \epsilon_2^2 \sim (T - T_C)^{-2}$), while in the F phase the additional contribution ($\sim (T - T_C)^{-1/2}$) to Δf_{222}^* gives also the first term of equation (13). Under applied hydrostatic pressure the maximum value of dielectric permittivity at T_C decreases (see corresponding results for CDP crystals obtained by Yasuda *et al* 1978), which manifests itself in an essential decrease of the electroacoustic effect in the N–F PT. This is in good agreement with our experimental data.

5. Conclusion

We have investigated the influence of hydrostatic pressure on the temperature behaviour of USW velocities and attenuations near the PT in DCDP and DRDP compounds. The P–T phase diagram of DCDP crystals obtained from these measurements is in good agreement with previous studies performed by Gesi and Ozawa (1978). Particularly, the triple point that separates N, F and AF phases has been found at $P_t = 575$ MPa and $T_t = 214$ K. These values of P_t and T_t differ only slightly from those obtained by Gesi and Ozawa (1978) and Marchon and Novak (1984), which is probably caused by the different value of the deuterium concentration in the specimens. In the case of DRDP crystals the obtained P–T phase diagram is in good agreement only with results of dielectric measurements performed earlier by Gesi *et al* (1983). No additional anomalies associated with pressure-induced PT have been observed in these crystals at high pressures in spite of previous studies by Baranov *et al* (1985). The results obtained are considered in the framework of phenomological theory. Using the group-theory method it is shown that PT into proper F and AF phases in DCDP crystals are connected with condensation of soft modes in the centre ($q_7 = 0$) or at the boundary ($q_{11} = b_1/2$) of the Brillouin zone, respectively. The soft modes in both cases transform according to one-dimensional irreducible representation A_u. This irreducible representation is also responsible for the PT from the N to the IM phase ($T = T_1$) in DRDP crystals. At the same time, it is impossible to explain the change of symmetry ($P2_1/c \to P2_1$) in the second-order PT and the appearance of uncompensated homogeneous polarization by the condensation only of the single soft mode at $q_{11} = \tfrac{1}{2} b_1$ near the PT from the IM to the FI phase. Similarly to the case of the betaine calcium chloride dihydrate (BCCD) compound (Dvorak 1990), we propose the two-soft-modes model,

according to which two modes $R(q_{11} = \frac{1}{2}b_1) \in B_g$ and $R(q_{11} = \frac{1}{2}b_1) \in B_u$ both condensed *simultaneously near the same* PT *temperature* T_2. The explanation of the acoustic properties near all the PT in DCDP and DRDP crystals is given in the framework of the frequently used previous phenomenological model (see for example Rehwald 1973) where the third- or fourth-order anharmonic interactions between the strains and the above normal soft-mode phonon coordinates are taken into account. The experimental results clearly indicate significant increase of the fluctuation effects near the triple point of DCDP crystals. These effects we attribute to antipolarization fluctuations, which earlier have been observed in Raman spectra by Marchon and Novak (1984). Note that the significant influence of fluctuation on the acoustic properties in the N phase takes place also in DRDP crystals already at atmospheric pressure.

We have investigated the influence of hydrostatic pressure on the temperature dependences of linear electroacoustic coefficient f^*_{222} near the PT in DCDP crystals. The phenomenological analysis clearly shows that the anomalous temperature behaviour of the linear electroacoustic effect near the N–F PT is caused mainly by the temperature dependence of the dielectric susceptibility ϵ_2 near T_C.

References

Baranov A I, Ivanov N R, Sandler V A, Fedosyuk R M and Yajushkin E D 1985 *Ferroelectrics* **63** 91

Dvorak V 1990 *Ferroelectrics* **104** 135

Frazer B C, Semmingsen D, Ellenson W D and Shirane D 1979 *Phys. Rev.* B **20** 2745

Geguzina S and Krivoglaz M 1967 *Fiz. Tverd. Tela* **9** 3095

Gesi K and Ozawa K 1978 *Japan. J. Appl. Phys.* **17** 435

Gesi K, Ozawa K, Osaka T and Makita Y 1983 *J. Phys. Soc. Japan* **52** 2538

Hagiwara B T, Itoh K, Nakamura E, Komukae M and Makita Y 1984 *Acta Crystallogr.* C **40** 718

Itoh K, Hagiwara T and Nakamura E 1983 *J. Phys. Soc. Japan* **52** 2626

Iwata Y, Koyano N and Shibuya I 1980 *J. Phys. Soc. Japan* **49** 304

Kanda E, Tamaki A, Jamaki T and Fujimura T 1983 *J. Phys. Soc. Japan* **52** 3085–92

Kasahara M, Aoki M and Tatsuzaki I 1984 *Ferroelectrics* **55** 47

Komukae M and Makita Y 1985 *J. Phys. Soc. Japan* **54** 4359

Kovalev O V 1986 *Neprivodimye i Inducirovannye Predstavleniya i Copredstavleniya Fedorovskih Grup* (Moscow: Nauka)

Levanyuk A, Minajeva K and Strukov B 1968 *Fiz. Tverd. Tela* **10** 2443

Marchon B and Novak A 1984 *Ferroelectrics* **55** 55

Papadakis E P 1967 *J. Acoust. Soc. Am.* **42** 1045

Rehwald W 1973 *Adv. Phys.* **22** 721

Semmingsen D, Ellenson W D, Frazer B C and Shirane D 1977 *Phys. Rev. Lett.* **38** 1299

Semmingsen D and Thomas R 1978 *Acta Crystallogr.* **34** S293

Smolenskiy G A, Bokov V A, Isupov V A, Krajnik N N, Pasunkov R E, Sokolov A I and Yushin N K 1985 *Fizika Segnetoelectricheskich Javlenii* (Leningrad: Nauka)

Sumita M, Osaka T and Makita Y 1981 *J. Phys. Soc. Japan* **50** 154

Suzuki S, Arai K, Sumita M and Makita Y 1983 *J. Phys. Soc. Japan* **52** 2394

Wada M, Sawada A and Ishibashi Y 1979 *J. Phys. Soc. Japan* **47** 1571

Yakushkin E D 1986 *Crystallografia* **31** 606

Yasuda N, Okamoto M, Shimuzu H, Fujimoto S, Yoshino K and Inuishi Y 1978 *Phys. Rev. Lett.* **41** 1311

Youngblood R, Frazer B C, Eckert J and Shirane G 1980 *Phys. Rev.* B **22** 228